Journal of Physiology (1990), **422**, *pp.* 203–225
With 13 *figures*
Printed in Great Britain

ANALYSIS OF EXCITATORY SYNAPTIC ACTION IN PYRAMIDAL CELLS USING WHOLE-CELL RECORDING FROM RAT HIPPOCAMPAL SLICES

BY S. HESTRIN*, R. A. NICOLL†, D. J. PERKEL† AND P. SAH†

*From the *Department of Physiology and the †Departments of Pharmacology and Physiology, University of California, San Francisco, CA 94143, USA*

(*Received 29 April 1989*)

SUMMARY

1. The pharmacological and biophysical properties of excitatory synapses in the CA1 region of the hippocampus were studied using patch electrodes and whole-cell recording from thin slices.

2. Excitatory postsynaptic currents (EPSCs) had a fast component whose amplitude was voltage insensitive and a slow component whose amplitude was voltage dependent with a region of negative slope resistance in the range of −70 to −30 mV.

3. The voltage-dependent component was abolished by the *N*-methyl-D-aspartate (NMDA) receptor antagonist DL-2-amino-5-phosphonovalerate (APV; 50 μM), which had no effect on the fast component. Conversely, the fast voltage-insensitive component was abolished by the non-NMDA receptor antagonist 6-cyano-7-nitroquinoxaline-2,3-dione (CNQX; 10 μM) which had no effect on the slow component.

4. In Ringer solution with no added Mg^{2+} the current–voltage relation of the NMDA component was linear over a much larger voltage range than in the presence of 1·3 mM-Mg^{2+}.

5. The NMDA component of the EPSC could be switched off with a hyperpolarizing voltage step at the soma. The kinetics of this switch-off was used to estimate the speed of clamp control of the subsynaptic membrane as well as the electrotonic distance from the soma. The kinetic analysis of the EPSC was restricted to synapses which were judged to be under adequate voltage control.

6. For those synapses that were close to the soma the time constant for decay for the non-NMDA component, which was voltage insensitive, ranged from 4–8 ms.

7. The rise time for the NMDA component was 8–20 ms and the time constant for decay ranged from 60–150 ms.

8. During increased transmitter release with post-tetanic potentiation or application of phorbol esters, both components of the EPSC increased to a similar extent.

9. These experiments provide a detailed description of the dual receptor mechanism operating at hippocampal excitatory synapses. In addition, the

MS 7663

experiments provide an electrophysiological method for estimating the electrotonic distance of synaptic inputs.

INTRODUCTION

It is now generally accepted that L-glutamate is the neurotransmitter acting at the various excitatory synapses in the hippocampus. It is also clear that in the vertebrate CNS, glutamate binds to at least three different types of receptors. These three receptor subtypes can be distinguished by their specific ligands quisqualate (quis), kainate and *N*-methyl-D-aspartate (NMDA) (Watkins & Evans, 1981). They can also be distinguished using specific receptor antagonists. Until quite recently, however, the only selective antagonist available was DL-2-amino-5-phosphonovalerate (APV), which competitively antagonizes the action of glutamate at the NMDA receptor. With APV, it has been possible to pharmacologically separate out the quis/kainate-receptor mediated component of glutamatergic EPSPs (Collingridge, Kehl & McLennan, 1983; Dale & Roberts, 1985; Collingridge, Herron & Lester, 1988*a*; Forsythe & Westbrook, 1988). The properties of the NMDA-mediated component have been inferred by subtraction of traces before and after application of APV. Recently a new compound, CNQX, has become available which is a specific antagonist at non-NMDA receptors (Blake, Brown & Collingridge, 1988; Honoré, Davies, Drejer, Fletcher, Jacobsen, Lodge & Nielsen, 1988). It has thus become possible to directly examine the properties of NMDA-mediated synaptic potentials and currents. Using these compounds, it has been demonstrated that both NMDA and non-NMDA receptor types are activated during synaptic transmission at the Schaffer collateral–commissural to CA1 synapse (Blake *et al.* 1988; Kauer, Malenka & Nicoll, 1988; Muller, Joly & Lynch, 1988; Andreasen, Lambert & Jensen, 1989).

In order to understand the kinetics of the conductance changes that underlie synaptic transmission, it is essential to be able to voltage clamp the postsynaptic membrane (Magleby & Stevens, 1972; Brown & Johnston, 1983; Finkel & Redman, 1983; Johnston & Brown, 1983; Nelson, Pun & Westbrook, 1986). This is particularly true for excitatory synaptic responses which can be voltage dependent and have reversal potentials far from the resting membrane potential. Voltage clamp analysis has been difficult in mammalian CNS because of the problems associated with voltage clamping small cells with extended dendritic structures (Brown & Johnston, 1983; Johnston & Brown, 1983). For this reason, quantitative studies of excitatory amino acid transmission have largely been limited to invertebrate and cultured systems (see Mayer & Westbrook, 1987).

In this paper we have used a new technique in which neurones in thin slices of brain can be studied using conventional patch clamp techniques (Edwards, Konnerth, Sakmann & Takahashi, 1989). We report here the properties of the conductance changes that occur at the Schaffer collateral–commissural to CA1 synapse in rat hippocampus.

METHODS

All experiments were performed on slices of adult rat hippocampi. Rats were anaesthetized with halothane and decapitated with a guillotine. The brain was rapidly removed and placed in cold

oxygenated mammalian Ringer solution. The brain was then hemisected and a cut was made above the corpus callosum at right angles to the surface of the midbrain. This cut surface was then glued to the stage of a vibratome (Lancer) using cyanoacrylate glue (Krazy Glue). Thin slices (100–120 μm) of hippocampus and surrounding cortex were then cut. The stage of the vibratome was bathed in ice-cold Ringer solution during the cutting procedure. Usually ten to twelve slices could be obtained from a single hemisphere. Slices were then maintained at room temperature in oxygenated Ringer solution (see below).

After a 1 h incubation period single slices were transferred as needed to the recording chamber and held down with a nylon net stretched out on a U-shaped piece of flattened platinum wire (Edwards *et al.* 1989). The chamber was then mounted onto the stage of a microscope and pyramidal neurones in the CA1 region visualized using Nomarski optics at a magnification of $\times 800$. A water-immersion $\times 40$ objective (Zeiss) with a numerical aperture of 0·75 was used. The slice was continuously perfused with normal oxygenated Ringer solution which consisted of (in mM): NaCl, 119; KCl, 2·5; $MgSO_4$, 1·3; $CaCl_2$, 2·5; NaH_2PO_4, 1; $NaHCO_3$, 26·2; glucose, 11; Na-HEPES, 10. The pH of the Ringer solution was 7·2. Glycine (1 μM) was routinely added to the Ringer solution to ensure a constant, saturating concentration of glycine for the NMDA receptor. In addition this minimized the antagonism by CNQX of NMDA responses (Lester, Quarum, Parker, Weber & Jahr, 1989). Under these conditions many cells could be seen to have 'clean' surfaces on the surface of the slice. Cells deeper in the slice could also be recorded from once the overlying tissue was removed using a pipette filled with Ringer solution to blow away the tissue (Edwards *et al.* 1989).

Whole-cell pipettes were filled with an intracellular solution of the following composition: CsF, 130; NaCl, 10; Na-EGTA, 10; Na-HEPES, 10; pH 7·2. In some cases CsF was replaced with KF. Caesium was chosen as the main cation in order to block potassium conductances. Fluoride was chosen as the main anion because it has been shown to reduce calcium currents (Kostyuk, Krishtal & Pidoplichko, 1975; Kay, Miles & Wong, 1986) and secondly because it improved the duration of the recordings. We have also used potassium phosphate and KCl in the intracellular solution. No differences were found with these solutions.

The Schaffer collateral–commissural fibres were stimulated with an isolated stimulator. The stimulating electrode consisted of two stainless-steel electrodes (Frederick Haer) glued 250 μm apart inserted into s. radiatum. In most experiments the electrode near the soma (within 50 μm) was the cathode. In other experiments two indifferent electrodes were placed in the bath and the two electrodes in the tissue were cathodes. This procedure was used to stimulate two separate pathways at different distances from the soma. The independence of the two pathways was verified by demonstrating that the current from the two pathways summated. GABA-mediated chloride currents were blocked by including 100 μM-picrotoxin in the superfusing solution. Excitatory postsynaptic potentials and currents (EPSPs and EPSCs) were recorded using a patch clamp amplifier (List Electronics, EPC-7). Currents were filtered at 2 kHz (8-pole Bessel filter, Frequency Devices) and recorded on line using an LSI 11/23 computer (DEC). Data was analysed off-line on a microVax II. The rise times were measured at the 10–90 % peak. The synaptic currents recorded were no larger than 300 pA and the measured series resistance was approximately 7 MΩ. The combined voltage error due to the leak current and synaptic current flowing through the series resistance was estimated to be less than 5 mV. EPSCs could be recorded in most cells and were routinely stable for more than an hour. EPSCs were usually elicited at a frequency of 0·2 Hz. All values are given as ± 1 standard deviation. All traces shown are averages of two to five traces unless otherwise stated.

Drugs used were tetrodotoxin (TTX, Sigma), 6-cyano-7-nitroquinoxaline-2,3-dione (CNQX, Tocris or CRB), phorbol 12,13-diacetate (Sigma) and DL-2-amino-5-phosphonovalerate (APV, CRB).

RESULTS

Whole-cell recordings were obtained from 178 pyramidal neurones. Figure 1*A* and *B* illustrates some of the properties of one of these cells perfused internally with KF. The cell was held at -85 mV and depolarizing current pulses injected (Fig. 1*A*) which evoked an action potential of > 90 mV. In cells perfused with CsF the input impedance was 200–900 MΩ. Under voltage clamp small voltage steps produced

capacitative transients that could be fitted with the sum of two or more exponentials as expected for a cell with an extended dendritic structure. One example which has been fitted with two exponentials is shown in Fig. 1*C*. EPSPs (Fig. 1*B*) could be evoked by stimulating the Schaffer collateral–commissural fibres. EPSCs recorded at −90 mV (Fig. 1*D*) ranged in size from about 10 to several hundred pA depending upon the stimulus strength. These currents were blocked by TTX (1 μM), cadmium

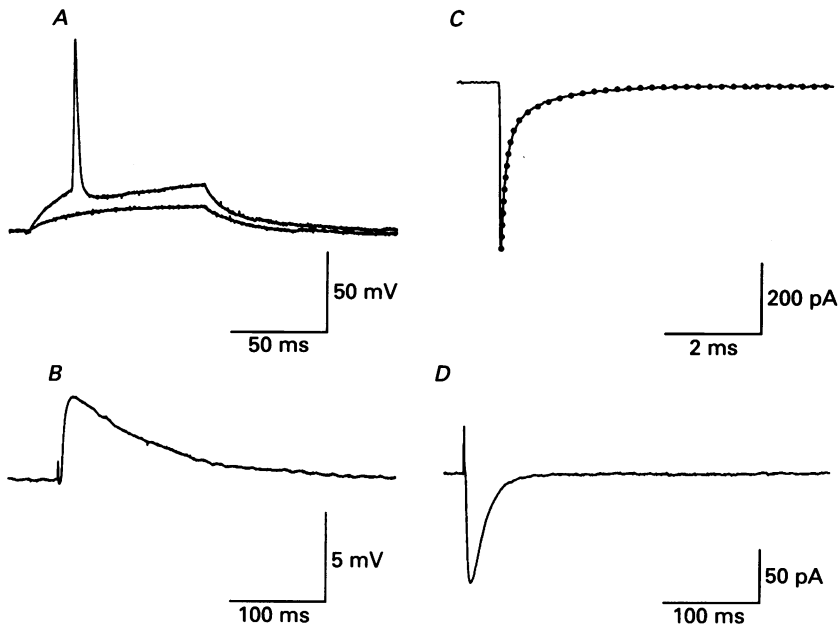

Fig. 1. Tight-seal whole-cell recording from CA1 pyramidal neurones in thin slices. *A* and *B*, current clamp recording. *A*, voltage response to depolarizing currents of 20 and 40 pA. The holding membrane potential was −85 mV. The internal solution was KF. *B*, EPSP evoked in response to stimulation of Schaffer collateral–commissural fibres in the same cell at the same holding potential. *C* and *D*, voltage clamp recording. *C*, capacitative transients generated by a 10 mV hyperpolarizing step from a holding potential of −90 mV. The dotted line is the fitted double-exponential function with time constants of 9·3 and 0·9 ms. *D*, EPSC evoked in response to stimulation of the excitatory afferents at −90 mV.

(100 μM) and the non-specific glutamate antagonist kynurenic acid (0·5 mM), thus confirming that the EPSCs are indeed generated by stimulation of the distal axon stumps of the Schaffer collateral–commissural fibres.

Pharmacological properties of EPSC

EPSCs recorded over a range of membrane potentials are illustrated in Fig. 2*A*. As the membrane potential is depolarized a slow component to the EPSC becomes apparent. In order to examine the two components we measured the peak current–voltage (*I–V*) relation as well as the *I–V* relation at 25 ms after the peak of the EPSC (dotted line in Fig. 2*A*). The peak *I–V* relation (▲ in Fig. 2*B*) is linear over the whole voltage range with a reversal potential of 0 mV whereas the *I–V* relation

measured 25 ms after the peak (●) is non-linear with a region of negative slope resistance in the range −70 to −30 mV. These properties of the two components of the EPSC are similar to those reported from other preparations (Collingridge *et al.* 1983; Dale & Roberts, 1985; Collingridge *et al.* 1988*a*; Forsythe & Westbrook, 1988). In order to examine the two components of the EPSC in isolation we used the two selective antagonists APV and CNQX. Although it is not possible to distinguish

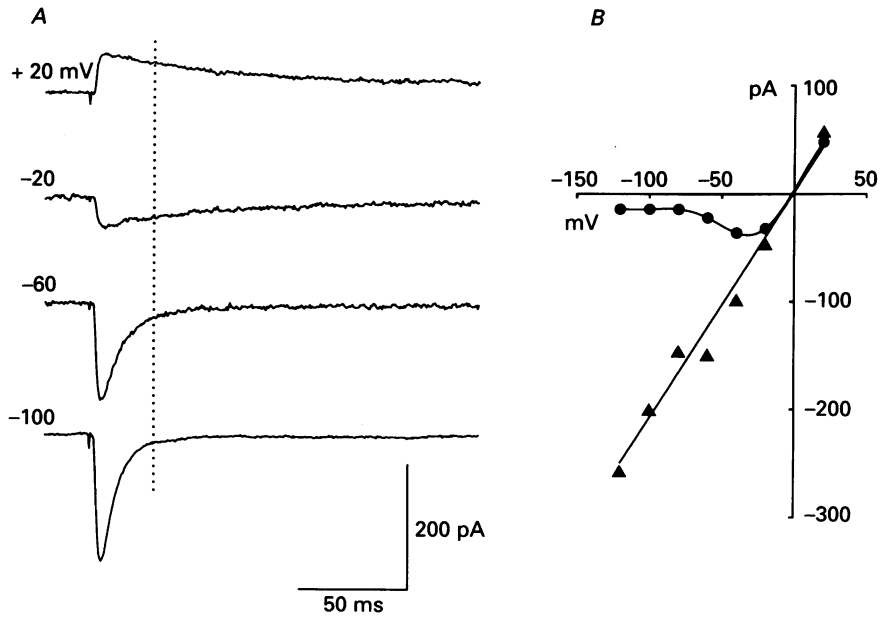

Fig. 2. The voltage-dependent properties of the EPSC. *A*, the EPSC was recorded at the indicated membrane potentials. *B*, the currents measured at the peak of the EPSC (▲) and at 25 ms after the peak (●, dotted line in *A*) are plotted in relation to the membrane potential.

pharmacologically between involvement of quis or kainate receptors in the non-NMDA component of the EPSC, quis receptor binding is approximately 10-fold higher than kainate receptor binding in s. radiatum in CA1 (Monaghan, Nguyen & Cotman, 1986; Westerberg, Monaghan, Kalimo, Cotman & Wielock, 1989). Thus for simplicity we will refer to the non-NMDA component as the quis component.

The effect of the selective NMDA blocker DL-APV (50 μM) is illustrated in Fig. 3*A*. At hyperpolarized membrane potentials, APV ($n = 23$) has no effect on the EPSC while at depolarized potentials APV completely abolishes the slow component of the EPSC. This effect was fully reversible (not shown). The peak *I–V* relation as well as that recorded 25 ms after the peak for this cell before and after addition of APV is shown in Fig. 3*B*. APV ($n = 5$) completely blocks the negative slope conductance measured at 25 ms. The remaining conductance in APV is linear and due to the small residual quis component remaining at 25 ms.

The component of the EPSC mediated by NMDA receptors can be examined in isolation in the presence of the selective non-NMDA blocker CNQX (10 μM) (Fig. 4).

In contrast to the effect of APV, CNQX essentially abolished the EPSC at hyperpolarized potentials, as expected since no NMDA component is present at these potentials (Mayer, Westbrook & Guthrie, 1984; Nowak, Bregestovski, Ascher, Herbet & Prochiantz, 1984; Kauer *et al.* 1988; Muller *et al.* 1988), while having only a small effect at depolarized potentials (Fig. 4*A*). The slow component was unaffected

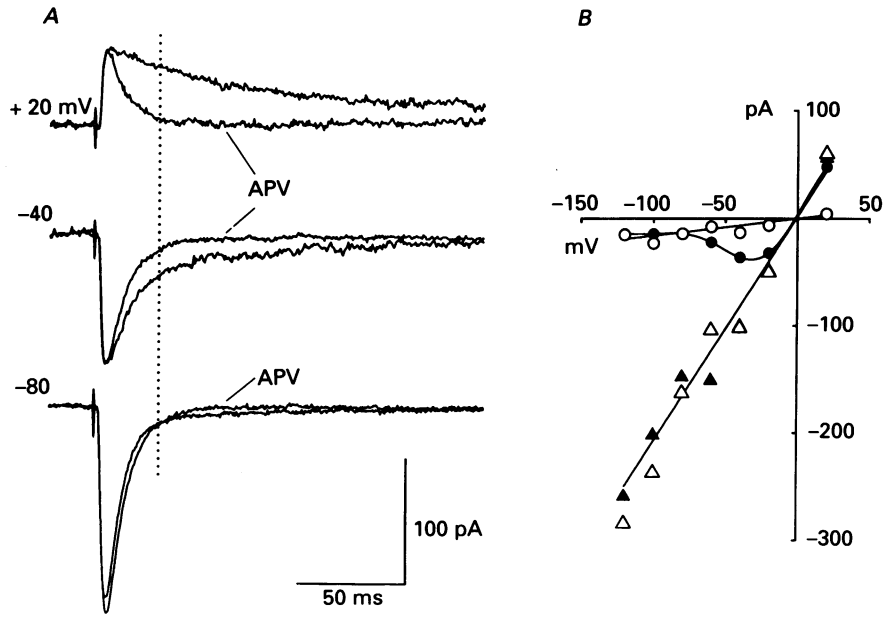

Fig. 3. The effect of APV. *A*, the EPSC was recorded before and during the application of 50 μM-DL-APV at the indicated membrane potentials. *B*, peak current–voltage relations are shown before (▲) and during (△) the application of APV. The current–voltage relation measured 25 ms after the peak of the EPSC (dotted line in *A*) before (●) and during (○) application of APV are also shown.

by CNQX. The synaptic current remaining in the presence of CNQX was abolished by adding 50 μM-APV (not illustrated), indicating that it is entirely mediated by an NMDA receptor. It should be noted that the rise time of the EPSC is dramatically slowed by CNQX. In six cells voltage clamped at −40 mV the rise time of the EPSC changed from 2·4 ± 0·6 to 11·8 ± 4·9 ms after application of CNQX.

The peak *I–V* relation measured in control solution is shown in Fig. 4 (▲, Fig. 4*B*). The *I–V* relation measured at 25 ms before (●) and during (○) CNQX application is shown in Fig. 4*B*. In the control solution the peak *I–V* is linear. In CNQX, as expected for the NMDA component, the *I–V* has a region of negative slope resistance between −70 and −20 mV ($n = 8$). It can also be seen that CNQX blocks the residual quis component measured at 25 ms.

The voltage-dependent nature of NMDA responses has been shown to result from a voltage-dependent blockade of the channel by extracellular magnesium (Mayer *et al.* 1984; Nowak *et al.* 1984). In order to examine the NMDA component over a wider voltage range, Mg^{2+} was removed from the bathing solution and CNQX added to remove the non-NMDA component ($n = 4$). NMDA EPSCs in this 'nominally Mg^{2+}-

free' Ringer solution are shown at two potentials in Fig. 5*A* and *B*. When Mg^{2+} (1·3 mM) is added, the response at −80 mV is markedly reduced whereas at +20 mV the reduction is much smaller. The peak *I–V* relation of the EPSC before (●) and after (○) addition of Mg^{2+} is shown in Fig. 5*C*. The *I–V* relation in Mg^{2+}-free Ringer solution is linear over a much larger voltage range but still displays a region of

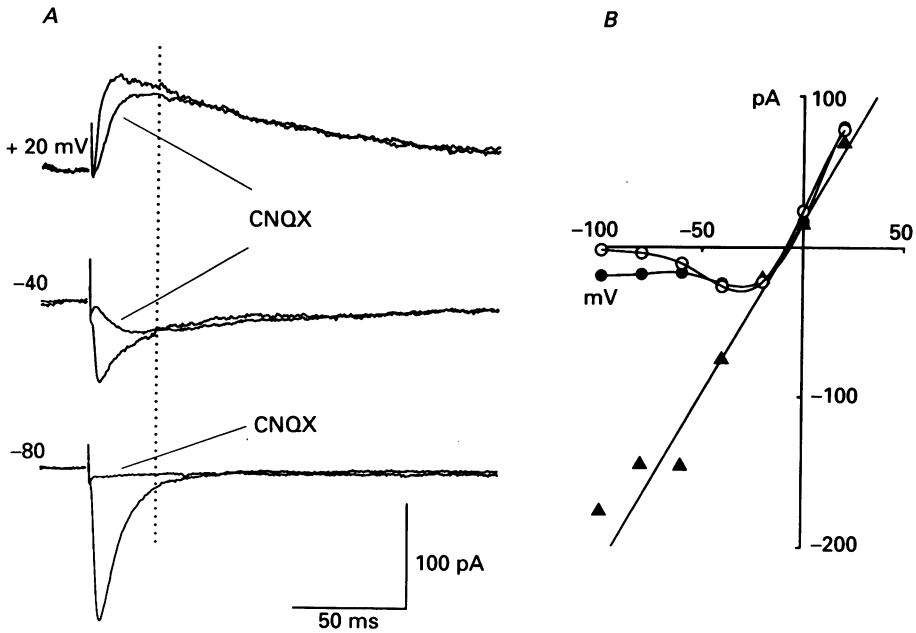

Fig. 4. The effect of CNQX. *A*, the EPSC was recorded before and during the application of 10 μM-CNQX at the indicated membrane potentials. *B*, Peak current–voltage relation in control solution (▲) and current–voltage relation measured 25 ms after the peak of the EPSC (dotted line in *A*) before (●) and during (○) application of CNQX.

negative slope resistance at very hyperpolarized potentials suggesting that there was still some Mg^{2+} remaining in the slice. The addition of Mg^{2+} will not only cause a voltage-dependent block of the NMDA channels but will also reduce transmitter release (del Castillo & Katz, 1954). This may account for the reduction in the synaptic current recorded at +20 mV. In Fig. 5*D* the peak conductance of the NMDA component is plotted against membrane potential for the cell shown in Fig. 4. The curve has been fitted with a Boltzmann equation where the half-maximal activation is −32 mV and for approximately 11 mV of depolarization the conductance increased e-fold. This value represents the voltage dependence of the Mg^{2+} block and is very close to that calculated for single NMDA channels (Ascher & Nowak, 1988*a*).

Kinetic properties of EPSC

Quis component

EPSCs measured in two different cells at −90 mV in normal extracellular Mg^{2+} are shown in Fig. 6*A*. The rise time of the two EPSCs is 1·7 and 4 ms, and the decays were

fitted with single-exponential functions and had time constants of 5·1 and 14·2 ms, respectively. In Fig. 6*B* the decay time constants are plotted against the rise time from sixty-one synapses. One explanation of the scatter is that the synapses are located at different distances from the soma and therefore filtered to different extents. Indeed, it was possible in the same cell to demonstrate a change in the time

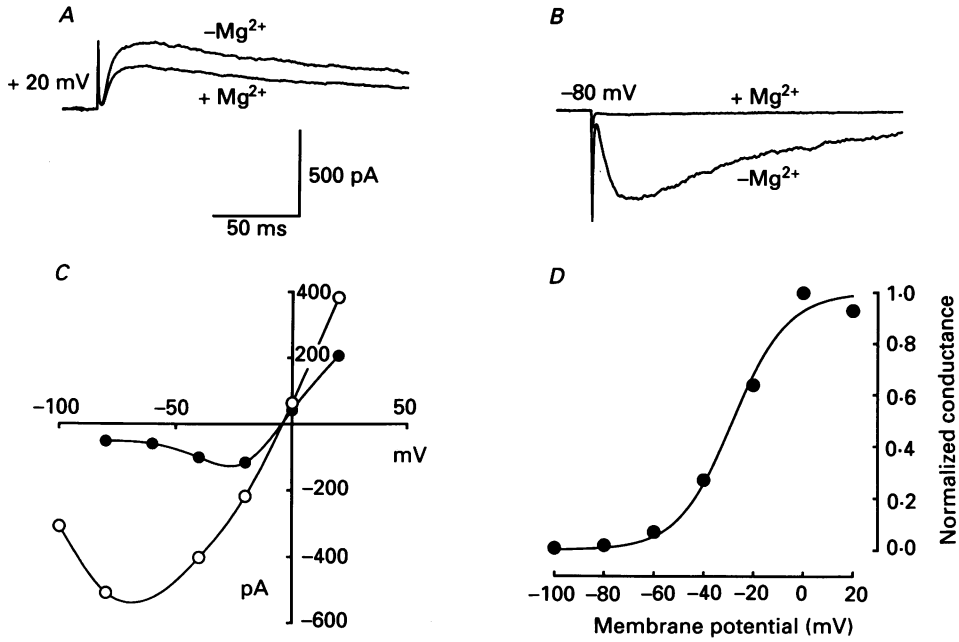

Fig. 5. Effects of external magnesium on the NMDA component recorded in CNQX. *A* and *B*, the EPSC recorded in control Ringer solution (1·3 mM-Mg^{2+}) and in nominally magnesium-free Ringer solution are shown at two different membrane potentials. *C*, the peak current–voltage relation in Mg^{2+}-free Ringer solution (○) and after the addition of Mg^{2+} (●). *D*, NMDA conductance–voltage relation. The peak NMDA conductance measured in the presence of CNQX was calculated by the equation $g = I/(V_0 - E_0)$. The continuous line through the points was drawn according to a Boltzmann relation.

course by positioning the stimulating electrode at different distances from the soma. In Fig. 6*B* the two lines connect values from synapses located 'near' and 'far' in the same cell. This suggests that the electrotonic structure of the cell and the location of the synaptic input can affect both the rise time and decay of the synaptic current recorded at the soma. Indeed for rise times greater than 3 ms there was a positive correlation between the rise time and the decay time constant. However, for rise times of less than 3 ms the decay time constant appeared to be independent of the rise time. These observations could be explained if the decay phase of these synapses is not appreciably filtered, whereas the rising phase, which is much faster, is significantly filtered. In addition, these results suggest that the voltage clamp control is adequate to measure the decay time constant in some but not all synapses. In order to interpret kinetic analyses it was thus important to evaluate further the voltage control of the subsynaptic membrane.

We calculated the average electrotonic length of the cells included in this study (L) to be $0{\cdot}72 \pm 0{\cdot}17$ ($n = 6$) which indicates that the steady voltage error could be as much as 20% at the distal end of the cable (see Appendix). Thus, to minimize this DC error we routinely activated synapses close to the soma. However, to analyse the time course of the EPSCs it is important, as discussed above, to evaluate the AC

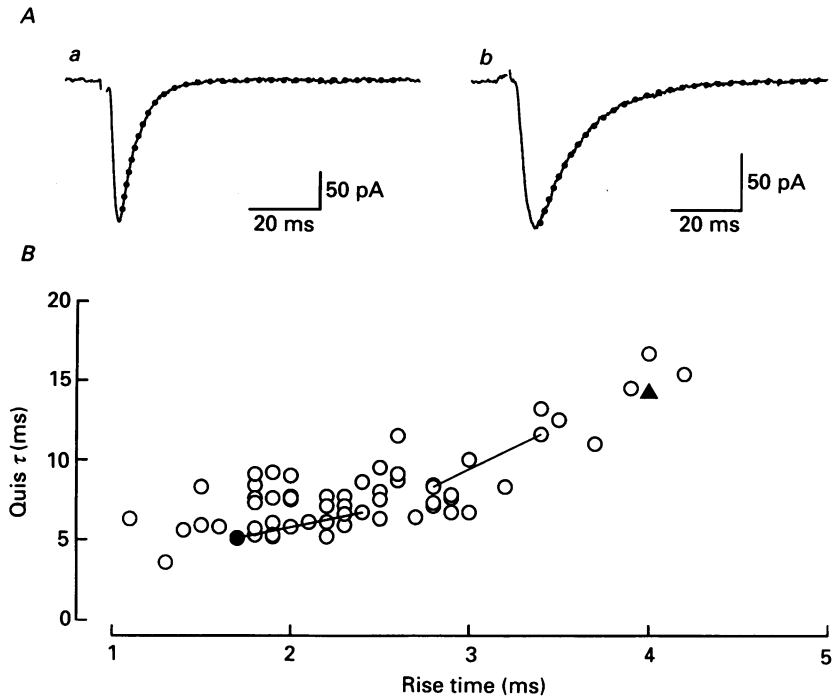

Fig. 6. The kinetics of the quis component. A, EPSCs recorded from two neurones at −90 mV. The rise times (10–90%) were 1·7 ms (Aa) and 4·0 ms (Ab). The dotted lines are single-exponential fits with time constants of 5·1 (Aa) and 14·2 ms (Ab). B, the rise times are plotted against the decay time constants of the quis components measured from sixty-one synapses. ● and ▲ represent the EPSCs shown in Aa and Ab respectively. The continuous lines in B indicate values obtained from the same cells at near and far synapses.

control of the membrane. This was tested using two types of experiments. The first type of experiment took advantage of the voltage-dependent nature of the NMDA component of the EPSC. The membrane potential was held at −40 mV and during an EPSC was stepped to −80 mV. Figure 7A shows the hyperpolarizing step alone and during an EPSC. Figure 7B shows the effect that the hyperpolarizing step has on the EPSC. Following the step, the EPSC decays back to the baseline with a time constant of 10 ms. It has previously been shown that the NMDA current is turned off with a time constant of 2–3 ms following a hyperpolarizing step (Mayer & Westbrook, 1985). Therefore a time constant slower than this must reflect the settling of the membrane potential at the synapse. In Fig. 7C the time constant for the switch-off of the NMDA component of the EPSC is plotted against the time constant of decay of the quis component (quis τ) for the same synapse ($n = 15$). For

values over 7·5 ms for the NMDA switch-off the quis τ is generally large and varies considerably among cells. In contrast, for values less than 7·5 ms the quis τ is relatively independent of the NMDA switch-off. This suggests that these values are not appreciably affected by the electrotonic structure of the cell (see Appendix). In

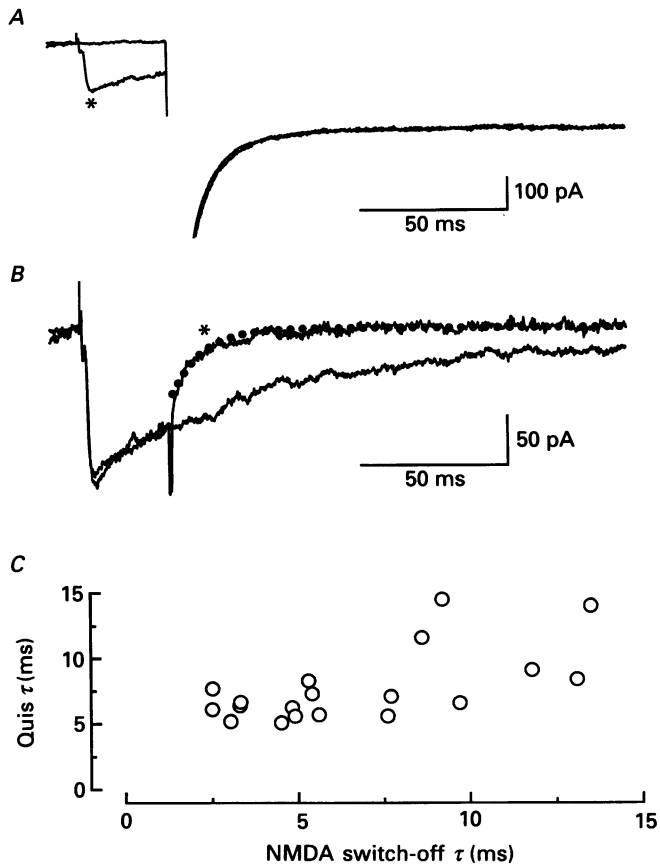

Fig. 7. The effect of a voltage jump on the time course of the NMDA component. *A*, the membrane current generated in response to a voltage step from −40 to −80 mV with (*) and without a preceding EPSC. *B*, subtraction of the traces in *A* revealed a time-dependent switch-off of the NMDA component (*). The dotted line is the single exponential fitted with a time constant of 10 ms. The synaptic current without the voltage jump is superimposed for comparison. *C*, the relation of the quis decay time constant to the kinetics of the NMDA switch-off measured from fifteen neurones. The quis τ was measured from single-exponential fits to EPSCs at −90 mV in the presence of Mg^{2+}. The NMDA switch-off was measured as illustrated in *A* and *B*.

the second type of experiment, the effect of a large hyperpolarizing step on the size of the quis EPSC was analysed (Fig. 8). The size of the EPSC was measured at −40 mV (S_1 in Fig. 8*A*) and at various intervals after the step to −100 mV (S_2 and S_3 in Fig. 8*A*) and compared to the EPSC measured with a holding potential of −100 mV (S_4 in Fig. 8*A*). The EPSC recorded at −40 mV is shown in Fig. 8*B* as S_1 and those measured at 3 and 5 ms are shown as S_2 and S_3. As the membrane potential settles

at the synapse to −100 mV the measured EPSC grows. It can be seen that the EPSC reached its final size within 5 ms.

These two types of experiments indicate that for synapses close to the soma the speed of the clamp is adequate to measure the decay time of the quis and NMDA

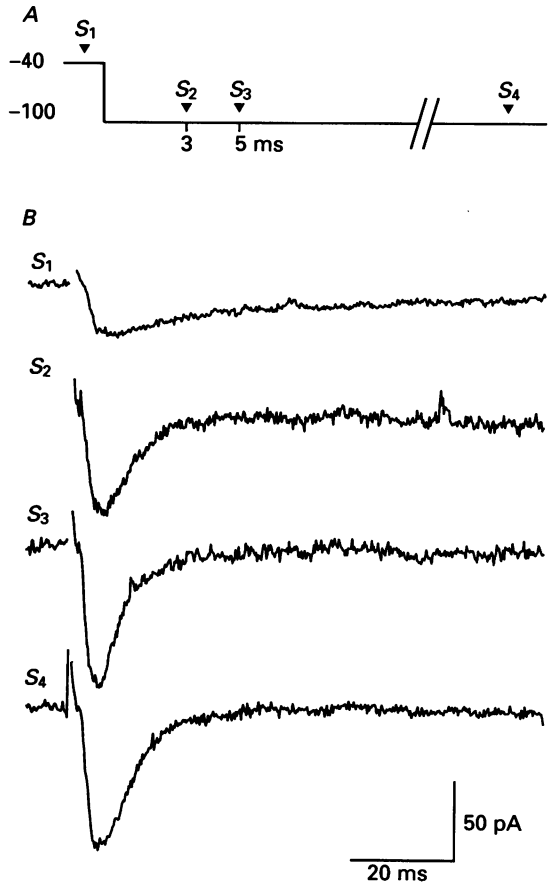

Fig. 8. The EPSC evoked at −40 mV (S_1) and 3 ms (S_2) and 5 ms (S_3) after a step to −100 mV. The EPSC evoked at a holding potential of −100 mV is indicated by S_4. Note that the amplitude of the EPSC evoked 3 ms after the voltage step (S_2) is 80% of that evoked at −100 mV (S_4).

synaptic components. It is also adequate to measure the rise time of the NMDA component but the rise time of the quis component will be appreciably filtered. For rise times of less than 3 ms the decay time constant averaged $7{\cdot}1 \pm 1{\cdot}6$ ms ($n = 54$). It should be noted that because the time constant of the NMDA component is much slower, it will not be significantly filtered. The voltage dependence of the time constant of decay of the quis component of the EPSC was examined in the presence of APV. Figure 9*A* shows an EPSC evoked at a series of membrane potentials. A single exponential has been fitted for each trace (see ○). In Fig. 9*B* these values are plotted against membrane potential and show that the decay is voltage insensitive.

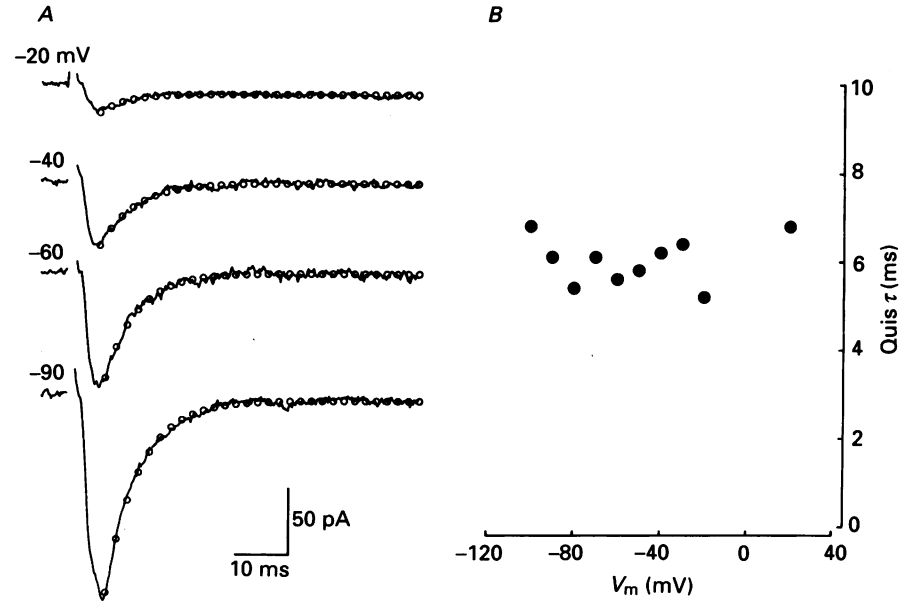

Fig. 9. Voltage dependence of the quis decay time constant. *A*, EPSC recorded in the presence of 50 μM-APV in one cell at the indicated membrane potentials. The ○ are the single exponentials fitted to the currents. *B*, the time constant of decay of the EPSC of the cell shown in *A* is plotted against the membrane potential.

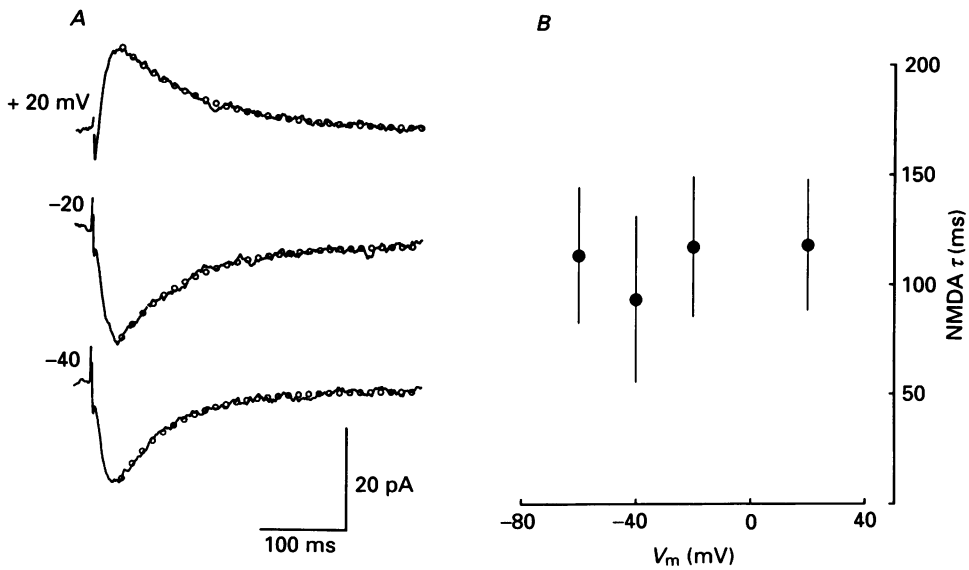

Fig. 10. Voltage dependence of the NMDA decay time constant. *A*, EPSC recorded in the presence of 10 μM-CNQX in normal Mg^{2+}-containing Ringer solution in one cell at the indicated membrane potentials. The time constant of decay was 65, 79 and 93 ms at −40, −20 and +20 mV respectively. The open circles are the single-exponential fits to the currents. *B*, average time constant of decay measured from five cells plotted against membrane potential. The bars represent ±1 S.D.

NMDA component

The time constant of decay of the NMDA component of the EPSC was examined in the presence of CNQX. Figure 10*A* shows EPSCs evoked at −40, −20 and +20 mV. The decay of the EPSC was well fitted with a single exponential. Although in some cells there was a small increase in the time constant of decay with membrane

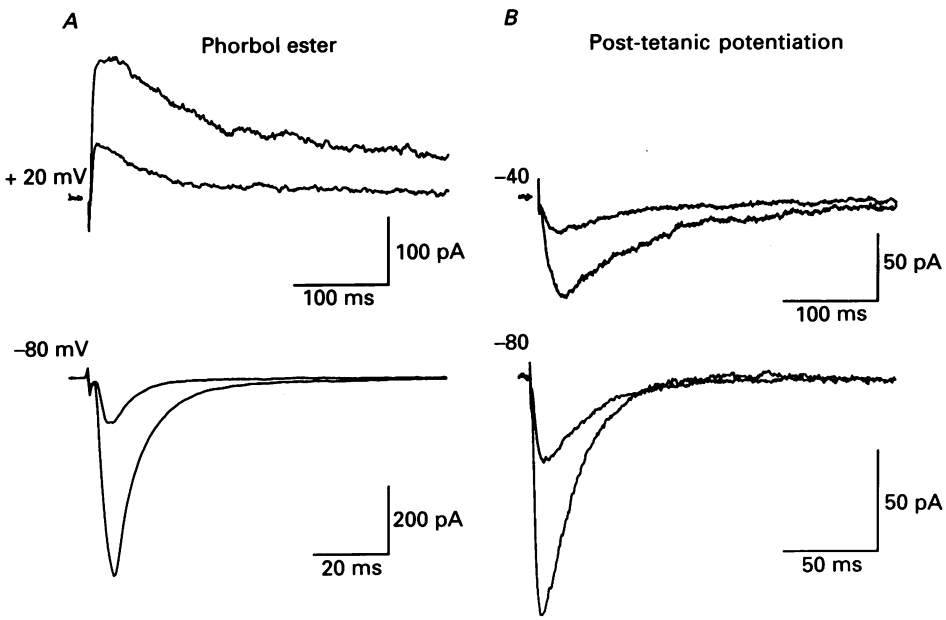

Fig. 11. Effect of increased transmitter release on EPSCs. *A*, effect of phorbol 12,13-diacetate (1 μM in 0·01 % DMSO) added to the normal Mg^{2+}-containing Ringer solution. The EPSCs evoked before and during application of phorbol ester are superimposed at the indicated membrane potentials. *B*, effect of high-frequency tetanus. The EPSCs evoked before and immediately after a high-frequency tetanus (100 Hz, 0·3 s) are superimposed at two membrane potentials. Note the different time bars. Both NMDA (+20, −40 mV) and quis (−80 mV) components are bigger after phorbol ester or tetanus.

depolarization (see Fig. 10*A*), no obvious voltage dependence could be seen in the average (see Fig. 10*B*). The average time constant of decay at −40 mV was 93 ± 38 ms ($n = 4$). Thus as in the case for the quis component of the EPSC the decay of the NMDA component of the EPSC is voltage insensitive.

In Fig. 11 the effect of increasing the release of glutamate from the synaptic terminals was examined. The cells were held either at −80 mV to examine the quis synaptic current or at a depolarized potential to unmask the NMDA synaptic component. Application of phorbol 12,13-diacetate (1 μM; $n = 3$) caused a large increase both in the quis and NMDA components (Fig. 11*A*). Likewise, following a high-frequency tetanus (30 stimuli at 100 Hz) both components were increased to a similar extent.

DISCUSSION

In this paper we have described some of the properties of the excitatory synapse between the Schaffer collateral–commissural fibres and CA1 pyramidal neurones in the adult rat hippocampus. To obtain quantitative data on synaptic properties it is essential to measure the synaptic currents under voltage clamp conditions. In central neurones this is difficult because (1) the neurones are small and have to be penetrated with high-resistance microelectrodes and (2) the extended geometry of the cell makes space clamp with a single electrode in the soma uncertain. Previous studies on excitatory synaptic action in hippocampal slices have used conventional intracellular recording with the single-electrode voltage clamp technique (Brown & Johnston, 1983; Collingridge *et al.* 1988*a*). This technique, though useful, is limited because of the high noise level and the poor current-passing capacity of intracellular microelectrodes, which means that the membrane potential can only be adequately controlled over a limited voltage range and for very small currents.

The application of the whole-cell tight-seal technique to these same neurones in slices offers an improvement in terms of the first difficulty mentioned above. Since the resistance of patch recording electrodes is considerably lower than conventional intracellular electrodes, the signal-to-noise ratio is larger and also larger currents can be passed through the electrode thus ensuring a 'faster' voltage clamp. In addition, being able to control the intracellular environment of the cell means that many voltage-dependent currents can be easily eliminated.

This technique, however, does not eliminate the problems of space clamp. As discussed in detail by Johnston & Brown (1983), in any voltage clamp study using electrodes in the soma, the limiting factor is the electrotonic structure of the cell. Whole-cell recording techniques offer an improved situation because (1) the electrode–cell seal is much higher than with a conventional microelectrode and (2) it is possible to perfuse the cell interior with a solution which minimizes problems due to voltage-dependent conductances thus increasing the space constant of the cell. However, it is still essential to demonstrate both the DC and AC control of the specific synapse under study. In this study the DC control of the subsynaptic membrane was directly assessed by plotting the conductance of the NMDA synaptic current *versus* membrane potential. This measured voltage sensitivity is remarkably similar to that obtained from single-channel recording (Ascher & Nowak, 1988*a*). In addition, the peak of the NMDA *I–V* curve is close to that seen in other preparations (Ascher, Bregestovski & Nowak, 1988; Mayer & Westbrook, 1985). If the DC control had been inadequate the voltage sensitivity would have been less steep and the peak of the *I–V* relation would have been shifted to the left.

The data in Fig. 6, which show a lack of correlation between the rise time and decay time constant for synapses with rise times of less than 3 ms, suggest that the decay phase at these synapses is under good voltage control. To evaluate directly the AC control of the subsynaptic membrane we took advantage of the voltage dependence of the NMDA synaptic current by measuring the time constant of switch-off of the synaptic current following hyperpolarizing steps. The time constant of the NMDA switch-off provided us with a measurement of the speed at which the voltage at a distant synapse settles in response to the voltage step at the soma, allowing us

to estimate the electrotonic distance to the synapse. Using this analysis it is shown in the Appendix that, for two cells with time constants of decay of 4·3 ms in which a full analysis was carried out, the speed of the clamp is adequate to measure the time constant of decay. In addition, we measured the time required for the quis synaptic component to increase following a hyperpolarizing step (see Fig. 8). This latter procedure can be used in cases where the synaptic current does not contain a voltage-dependent component.

The quis component of the EPSC

Experiments with cultured CNS neurones have shown that the conductance activated by the quis and kainate receptors has a reversal potential close to zero with a linear single-channel current–voltage relation (Ascher & Nowak, 1988*b*; Cull-Candy, Howe & Ogden, 1988). However, the whole-cell current–voltage relation is non-linear at hyperpolarized membrane potentials (Mayer & Westbrook, 1984; Ascher & Nowak, 1988*b*). Our results indicate a linear current–voltage relation reversing at 0 mV.

The quis-, or CNQX-blockable component of the EPSC, had rise times of 1–3 ms. EPSCs measured in other preparations where the synapse is known to be close to or on the soma have times to peak of less than 1 ms (Finkel & Redman, 1983; Nelson *et al.* 1986). The most likely explanation for the slow time to peak in the present study is an inability of the clamp to follow the rising phase of the synaptic current.

The time course of decay of the adequately clamped EPSC followed an exponential time course and had a time constant of 7·1 ms. The time constant was insensitive to membrane potential over the voltage range −100 to +40 mV. Studies on quisqualate-activated single channels reveal a mean channel lifetime that ranges from 0·5 to 5·3 ms (Jahr & Stevens, 1987; Cull-Candy & Usowicz, 1989). Measurements from quisqualate-induced noise reveal two Lorentzians with mean channel lifetimes of 2 and 10–15 ms (Ascher & Nowak, 1988*b*; Cull-Candy *et al.* 1988; Cull-Candy & Usowicz, 1989). This raises the possibility that as demonstrated at the neuromuscular junction for the ACh receptor (Magleby & Stevens, 1972) the time constant of decay of the EPSC may reflect the mean open time of the quis channel. If this is indeed the case it indicates that the concentration of glutamate must fall very rapidly below the K_D for glutamate binding to the quis receptor (334 μM; Mayer, 1989). Yet as discussed below the glutamate concentration must remain high enough to continue to activate NMDA receptors. Desensitization of the quis receptor, which is known to be very fast to exogenously applied glutamate (Kiskin, Krishtal & Tsyndrenka, 1986; Trussell, Thio, Zorumski & Fischbach, 1988), provides another mechanism for the decay of the quis component of the EPSC (Tang, Dichter & Morad, 1989; Trussell & Fischbach, 1989). However, this finding is difficult to reconcile with the observation that concanavalin A reduces desensitization of quisqualate receptor responses but has no effect on the decay time constant of synaptic currents recorded in cultured cells (Mayer & Vyklicky, 1989).

This decay rate of the quis EPSC is slow in comparison to other synapses. At the primary afferent to motoneurone synapse, time constants of decay are 0·3–0·4 ms (37 °C, −70 mV) and decline with hyperpolarization (Finkel & Redman, 1983). In mouse spinal cord cultures a time constant of decay of 0·6 ms (at 25 °C), which was

voltage insensitive, is recorded (Nelson *et al.* 1986). At synapses between cultured hippocampal neurones, time constants around 1–4 ms (25 °C, −80 mV) have been reported (Forsythe & Westbrook, 1988). At the mossy fibre to CA3 input, Brown & Johnston (1983) measured a time constant of around 4 ms at −60 mV (32 °C) ms which decreased with depolarization. All these synapses are thought to use glutamate as the primary transmitter, raising the possibility that differences of the properties of the postsynaptic receptor/channel may exist at these different synapses.

The NMDA component

As reported before (Collingridge *et al.* 1988*a*; Forsythe & Westbrook, 1988), the NMDA component of the EPSC had a much slower rise time (8–20 ms) and a slower decay rate as well. The peak current–voltage relation showed the well-established region of negative slope resistance between −70 and −30 mV, with a reversal potential of 0 mV (Mayer *et al.* 1984; Nowak *et al.* 1984). The NMDA EPSC decayed in an exponential manner and had time constants of decay which ranged from 60 to 150 ms. No clear voltage sensitivity was observed for the time constant of decay. The reported open-time duration for NMDA channels is 5–10 ms (Cull-Candy & Usowicz, 1987; Jahr & Stevens, 1987; Ascher *et al.* 1988). There have been reports of burst openings lasting in excess of 100 ms (Jahr & Stevens, 1987; Howe, Colquhoun & Cull-Candy, 1988). However, the relative contribution of these long-lasting events to the total current is not known. Thus, it is not entirely clear if the time course of decay of the NMDA component reflects the concentration of glutamate at the synapse or the burst duration of the channel.

How can one explain the very different time courses of the quis and NMDA components? If we accept that the K_D for glutamate binding to the NMDA receptor (2·8 μM) is much lower than that for the quis receptor (Mayer, 1989), it is possible that the glutamate concentration falls to a subthreshold value for activating quis receptors at a faster rate than the decay of the quis component of the EPSC, implying that the decay of the quis component is determined by the single-channel properties. The concentration, however, would have to remain sufficiently high to activate NMDA receptors and the time course of the NMDA component of the EPSC would be determined by the concentration of glutamate. As a corollary this model suggests that the removal of synaptically released glutamate has two time constants. One clear problem in such a scheme is the slow rise time of the NMDA component of the EPSC, which occurs at a time when it is postulated that the glutamate concentration is actually falling. Thus to accept the scheme one must propose that a considerable delay exists in the opening of NMDA channels. Alternatively the slow kinetics of the rise time and decay could be explained if glutamate acted on perisynaptic NMDA receptors. At the present time it is not possible to distinguish between these two alternatives.

In the last set of experiments we have examined the effect on the EPSC of procedures that increase the release of glutamate. This includes the activation of protein kinase C by phorbol esters which is known to increase transmitter release at a variety of synapses (Peterfreund & Vale, 1983; Rink, Sanchez & Hallam, 1983; Pozzan, Gatti, Dozio, Vicentini & Meldolesi, 1984; Wakade, Malhotra & Wakade, 1985; Zurgil & Zisapel, 1985; Malenka, Ayoub & Nicoll, 1987; Shapira, Silberberg,

Ginsberg & Rahamimoff, 1987), including the excitatory synapses in the CA1 region of the hippocampus (Malenka *et al.* 1987) and post-tetanic potentiation, which is also associated with an increase in transmitter release (Zucker, 1989). In both cases the size of the EPSC was increased and the quis and NMDA components were increased to a similar extent. This indicates that as more glutamate is released, both receptor subtypes have access to this extra glutamate.

The striking difference in the time course of the quis and NMDA synaptic currents, coupled with the powerful disynaptic inhibition, which occurs just after the peak of the quis current, is well suited for the proposed role of these two receptors in the plasticity observed at these synapses (Dingledine, Hynes & King, 1986; Collingridge, Herron & Lester, 1988*a*,*b*; Wigström & Gustafsson, 1985, 1988). Because of the voltage dependence of the NMDA channel, little activation of the channel will occur with single stimuli. However, during repetitive stimulation inhibition will diminish (McCarren & Alger, 1985), summation of the NMDA component will occur and concomitant quis receptor activation and NMDA receptor activation will occur. These three factors will greatly facilitate the coupling of membrane depolarization and NMDA receptor activation.

APPENDIX

In order to estimate quantitatively the spatial and temporal properties of the voltage control achieved in the experiments reported above we constructed a compartmental model of two of the pyramidal cells from the study. Assuming passive membrane throughout the cells, we determined the best-fitting parameters for the model from that cell's response to a small hyperpolarizing voltage step. The control of membrane potential was then determined for a variety of circumstances, and we estimated the location of the experimentally recorded synapses. We find that there is significant filtering of signals arising in the distal dendrites, but that in the proximal dendrites of these cells, processes with time constants slower than about 2–3 ms should be accurately measured by the techniques used.

Assumptions and calibration

For simulation of specific experimental protocols, we used the MANUEL family of programs developed by Donald H. Perkel (Perkel & Perkel, 1985). These programs solve an initial-value problem associated with a set of coupled, ordinary, linear or non-linear (see below) differential equations. Numerical integration was performed using a modified fourth-order Runge–Kutta algorithm with a variable step size (Gear, 1971). These programs permitted simulation of many of the experiments actually performed and in addition allowed further characterization of the cable properties of the dendritic structure.

The model cell was assumed to have the structure illustrated in Fig. 12*A*. Each of the regions was isopotential and was connected to adjacent regions through ohmic resistances. The neurone consisted of a spherical soma and a single cylindrical cable representing a collapsed dendritic arborization (Rall & Segev, 1985). The cable was divided into ten compartments, and the electrode was represented by a region of high resistance and low capacitance, connected to the soma via a series resistance. An equivalent-cylinder model can be characterized by five parameters: soma diameter,

dendrite length, dendrite diameter, specific membrane resistivity and series resistance. We estimated the parameters that best described an individual pyramidal cell from the transient current response of that cell to a step change in electrode voltage from −90 to −95 mV. The model parameters were varied under control of

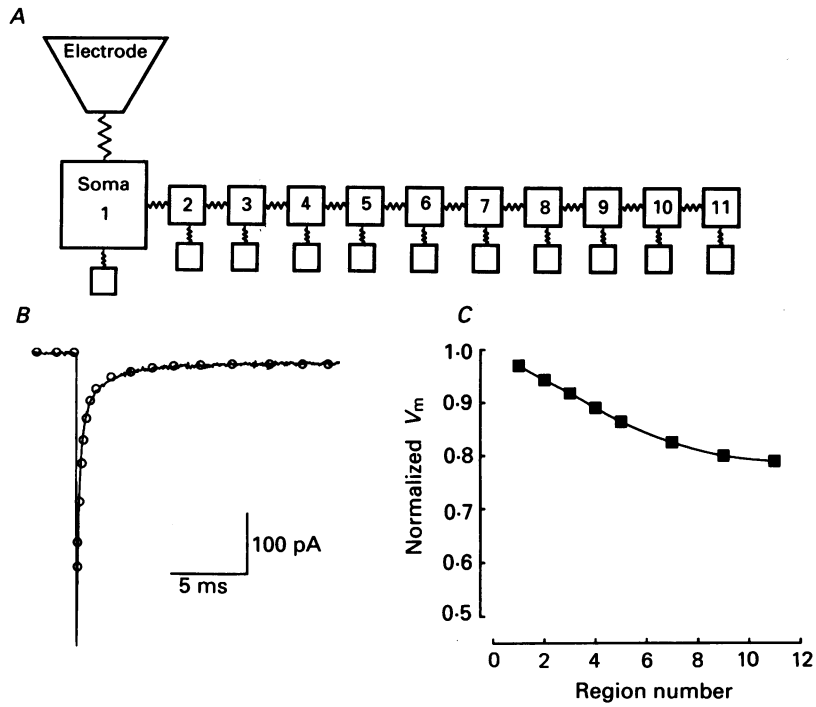

Fig. 12. Structure and calibration of the model cell. *A*, compartmentalization scheme for the pyramidal cell. The soma was connected to a series of ten dendritic regions, to each of which was attached a single dendritic spine. Each region (including the spines) was represented as a resistance and capacitance connected in parallel from cytoplasm to ground. Membrane areas, specific cytoplasmic resistivity, specific membrane resistivity and series resistance were adjusted so as to fit the response to a hyperpolarizing step from −90 to −95 mV (*B*). The resistance between the soma and most proximal dendritic region was assumed to be half that between more distal dendritic compartments. *C*, the quality of DC voltage control is illustrated with a plot of the steady-state voltage, normalized to the clamp potential in the electrode, as a function of distance from the soma. Cell 163.

a computer algorithm to find the set which minimized the difference between the recorded and model current traces. This method of estimating the cable properties of a neurone, termed the least-squares method, will be described in a future publication (S. Mittman & D. Copenhagen, unpublished observations). Extensive testing with simulated data has shown the method's reliability. The dendritic parameters obtained for the two cells are illustrated in Table 1, along with the compartmentalization values, which were determined from the assumed geometry. The specific cytoplasmic resistivity was assumed throughout to be 100 Ω cm (Jack, Noble & Tsien, 1983). The optimal dendritic parameters obtained using the least-squares method gave transient current responses that were very similar to the

recorded data (Fig. 12*B*); once the structural parameters were established for a given cell, they were not varied further except for the addition of a single dendritic spine with area of 1 μm^2 and a neck resistance of 100 MΩ on each of the dendritic regions (Jack *et al.* 1983).

Estimation of voltage control

Three different measurements were made of the characteristics of the voltage control: the steady-state voltage as a function of distance from the soma, the current

TABLE 1. Calibration parameters

Parameters from calibration	Cell 156	Cell 163
Soma diameter (μm)	23	23·6
Dendrite diameter (μm)	2·8	2·2
Dendrite length (μm)	682	705
Specific membrane resistivity ($k\Omega\ cm^2$)	16·1	20·7
Series resistance (MΩ)	9·7	11·1
Compartmentalization parameters		
Soma area (μm^2)	1660	1750
Area of each dendritic region (μm^2)	613	487
Membrane conductivity ($\mu S/cm^2$)	62·0	48·4
Resistance between dendritic regions (MΩ)	10·6	18·6

response to an instantaneous current impulse injected in a dendritic spine and the current response to a voltage step from −40 to −80 mV assuming a voltage-dependent conductance of the NMDA type in the head of a dendritic spine. These measurements then led to the possibility of estimating the current response to a conductance change approximating that of the quisqualate receptors during an EPSC.

When the electrode was clamped at −80 mV the steady-state voltage was calculated at different electrotonic distances, both in the dendritic shaft and in the spine head. These values are illustrated in Fig. 12*C*. The deviation of voltage from the clamp potential increases steadily with distance from the soma, and as expected for a terminated cable (Rall & Segev, 1984), tends to saturate in more distal segments (membrane potential in the most distal spine was −63 mV). All results illustrated are from cell 163, but those from cell 156 are qualitatively similar and support the same conclusion.

Two factors contribute to the time course of a measured EPSC: electrotonic distance between the synapse and the electrode, and time course of the underlying synaptic conductance. In order to separate the relative contributions of these two variables, we estimated the temporal filtering properties of the model cell. Under voltage-clamp conditions, the current response was calculated for instantaneous current impulses applied in dendritic spines at different distances from the soma. The use of such an infinitely brief stimulus allowed us to determine the influence of the cell's electrotonic structure on current waveforms spreading from the dendrite to the soma. The results are illustrated in Fig. 13*A*, in which responses to current impulses in proximal, intermediate and distal spines are superimposed. The time constants of decay of the currents as a function of distance are plotted as squares in Fig. 13*D*. It

is clear that with increasing distance from the soma, signals become more severely filtered.

Another characteristic of the voltage control in an extended structure is the time course of current flow and potential in the dendrites following a voltage step in the

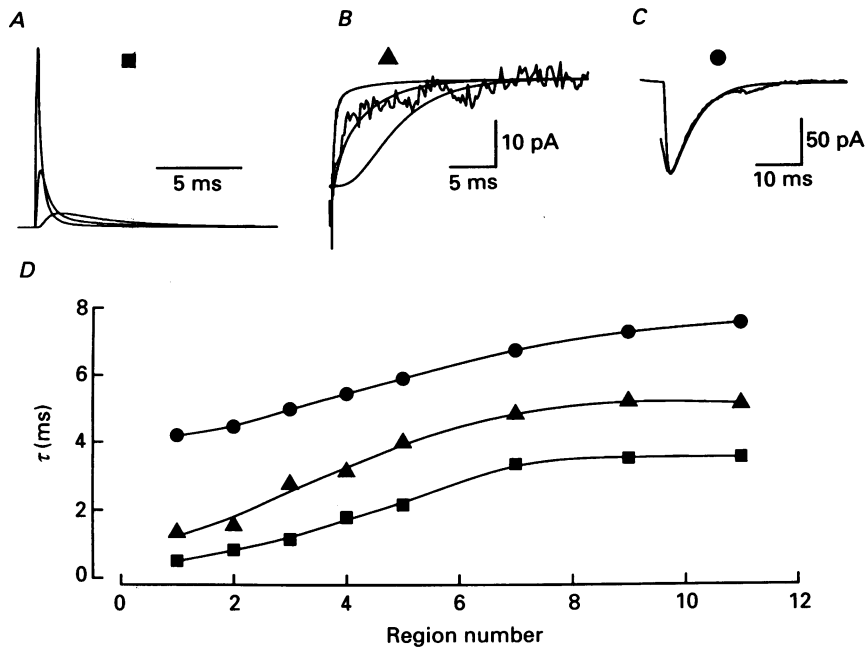

Fig. 13. *A*, characterization of the model cell using current impulses. Sample responses to a current impulse in the spines attached to regions 2, 4 and 9. The impulse consisted of a 20 mV hyperpolarization corresponding to the transfer of -2×10^{-14} C into the spine. *B*, switch-off of current through NMDA conductance following a voltage step from −40 to −80 mV. Superimposition of experimentally recorded current and those simulated for cases in which the voltage-dependent conductance was placed in the spine connected to region 2, 4, or 9. *C*, responses to a conductance change in dendritic spines. Superimposition of an experimentally recorded EPSC and that calculated for a conductance change with decay time constant of 4 ms in the spine connected to region 3. *D*, dependence of the decay time constants for current impulses (■), NMDA switch-offs (▲), and EPSCs (●) on distance from the soma. Cell 163.

electrode. We performed calculations of a simplified version of the 'switch-off' experiment described above. A conductance with voltage dependence similar to that of the NMDA conductance and time constant set at 0·1 ms was placed in the head of a single dendritic spine and the electrode clamped at −40 mV. The time course of the current response was then calculated following a step in the electrode from −40 to −80 mV (Fig. 13*B*). The difference in the currents recorded with active and passive membrane in the spine head represents the current flowing through the NMDA-type conductance as it would be recorded in the soma. The step hyperpolarization resulted in a greatly decreased conductance and the time course of the decaying current represents the combined filtering effects of the dendrites during both the propagation of the hyperpolarizing voltage step and the spreading

of the current back to the electrode from the spine. Near the soma, the reduction of the NMDA current took place with a time constant of approximately 1·8 ms. At more distal sites, however, the decay time constant increased with distance, reaching a final value of 5 ms in the most distal region. The relation between distance and time constant of decay is shown with triangles in Fig. 13*D*.

It appeared that in the proximal dendrites of the modelled cells the temporal characteristics of measured signals were significantly faster than the time constants of experimentally recorded EPSCs in these cells. We thus postulated that the measured values might reflect relatively accurately the true underlying conductance change. In order to test this idea, we applied a conductance change with a decay time constant of 4 ms in different regions, and calculated the current responses in the electrode. The simulated EPSC generated in the spine connected to region 3 resembled quite closely the observed EPSC ($\tau = 4{\cdot}4$ ms; Fig. 13*C*). As seen in Fig. 13*D* the time constant of the EPSC increased steadily with distance in the dendrite and appeared to reach a plateau in the most distal segments. In the proximal dendritic segments, thus, the time course of the measured EPSC provides a reasonable indication of the true conductance time course.

This work was supported by Grants MH-38256 (R.S.A.), MH-0037 and NS-24205 to R.A.N. and Grant EY07507 to S.H. We thank Dr F. Edwards for useful suggestions and S. Mittman for the use of software and his comments on the manuscript. The support of Dr J. I. Korenbrot is greatly appreciated.

REFERENCES

ANDREASEN, M., LAMBERT, J. D. C. & JENSEN, M. S. (1989). Effects of new non-*N*-methyl-D-aspartate antagonists on synaptic transmission in the *in vitro* rat hippocampus. *Journal of Physiology* **414**, 317–336.

ASCHER, P., BREGESTOVSKI, P. & NOWAK, L. (1988). *N*-Methyl-D-aspartate activated channels of mouse central neurones in magnesium free solutions. *Journal of Physiology* **399**, 207–226.

ASCHER, P. & NOWAK, L. (1988*a*). The role of divalent cations in the *N*-methyl-D-aspartate responses of mouse central neurones in culture. *Journal of Physiology* **399**, 247–266.

ASCHER, P. & NOWAK, L. (1988*b*). Quisqualate and kainate activated channels in mouse central neurones in culture. *Journal of Physiology* **399**, 227–245.

BLAKE, J. F., BROWN, M. W. & COLLINGRIDGE, G. L. (1988). CNQX blocks acidic amino acid induced depolarizations and synaptic components mediated by non-NMDA receptors in rat hippocampal slices. *Neuroscience Letters* **89**, 182–186.

BROWN, T. H. & JOHNSTON, D. (1983). Voltage-clamp analysis of mossy fiber synaptic input to hippocampal neurons. *Journal of Neurophysiology* **50**, 487–507.

COLLINGRIDGE, G. L., HERRON, C. E. & LESTER, R. A. J. (1988*a*). Synaptic activation of *N*-methyl-D-aspartate receptors in the Schaffer collateral–commissural pathway of rat hippocampus. *Journal of Physiology* **399**, 283–300.

COLLINGRIDGE, G. L., HERRON, C. E. & LESTER, R. A. J. (1988*b*). Frequency-dependent *N*-methyl-D-aspartate receptor-mediated synaptic transmission in rat hippocampus. *Journal of Physiology* **399**, 301–312.

COLLINGRIDGE, G. L., KEHL, S. J. & MCLENNAN, H. (1983). Excitatory amino acids in synaptic transmission in the Schaffer collateral–commissural pathway of the rat hippocampus. *Journal of Physiology* **334**, 33–46.

CULL-CANDY, S. G., HOWE, J. R. & OGDEN, D. C. (1988). Noise and single channels activated by excitatory amino acids in rat cerebellar granule neurones. *Journal of Physiology* **400**, 189–222.

CULL-CANDY, S. G. & USOWICZ, M. M. (1987). Multiple-conductance channels activated by excitatory amino acids in cerebellar neurons. *Nature* **325**, 525–528.

CULL-CANDY, S. G. & USOWICZ, M. M. (1989). Multiple conductances of glutamate receptor

channels. In *Allosteric Modulation of Amino Acid Receptors: Therapeutic Implications*, ed. BARNARD, E. A. & COSTA, E., pp. 265–285. Raven Press Ltd., New York.

DALE, N. & ROBERTS, A. (1985). Dual-component amino-acid-mediated synaptic potentials: excitatory drive for swimming in *Xenopus* embryos. *Journal of Physiology* **363**, 35–59.

DEL CASTILLO, J. & KATZ, B. (1954). The effect of magnesium on the activity of motor nerve endings. *Journal of Physiology* **124**, 553–559.

DINGLEDINE, R., HYNES, M. A. & KING, G. L. (1986). Involvement of *N*-methyl-D-aspartate receptors in epileptiform bursting in the rat hippocampal slice. *Journal of Physiology* **380**, 175–189.

EDWARDS, F. A., KONNERTH, A., SAKMANN, B. & TAKAHASHI, T. (1989). A thin slice preparation for patch clamp recordings from synaptically connected neurones of the mammalian central nervous system. *Pflügers Archiv* **414**, 600–612.

FINKEL, A. S. & REDMAN, S. J. (1983). The synaptic current evoked in cat spinal motoneurones by impulses in single group Ia axons. *Journal of Physiology* **342**, 615–632.

FORSYTHE, I. D. & WESTBROOK, G. L. (1988). Slow excitatory postsynaptic currents mediated by *N*-methyl-D-aspartate receptors on mouse cultured central neurones. *Journal of Physiology* **396**, 515–533.

GEAR, C. W. (1971). *Numerical Initial Value Problems in Ordinary Differential Equations*. Prentice-Hall, Englewood Cliffs, NJ, USA.

HABLITZ, J. J. & LANGMOEN, I. A. (1982). Excitation of hippocampal pyramidal cells by glutamate in the guinea-pig and rat. *Journal of Physiology* **325**, 317–331.

HONORÉ, T., DAVIES, S. N., DREJER, J., FLETCHER, E. J., JACOBSEN, P., LODGE, D. & NIELSEN, F. E. (1988). Quinoxalinediones: Potent competitive non-NMDA glutamate receptor antagonists. *Science* **241**, 701–703.

HOWE, J. R., COLQUHOUN, D. & CULL-CANDY, S. G. (1988). On the kinetics of large-conductance glutamate-receptor ion channels in rat cerebellar granule neurons. *Proceedings of the Royal Society* B **233**, 407–422.

JACK, J. J. B., NOBLE, D. & TSIEN, R. W. (1983). *Electric Current Flow in Excitable Cells*. Clarendon Press, Oxford.

JAHR, C. E. & STEVENS, C. F. (1987). Glutamate activates multiple single channel conductances in hippocampal neurones. *Nature* **325**, 522–525.

JOHNSTON, D. & BROWN, T. H. (1983). Interpretation of voltage-clamp measurements in hippocampal neurons. *Journal of Neurophysiology* **50**, 464–486.

KAUER, J. A., MALENKA, R. C. & NICOLL, R. A. (1988). A persistent postsynaptic modification mediates long-term potentiation in the hippocampus. *Neuron* **1**, 911–917.

KAY, A. R., MILES, R. & WONG, R. K. S. (1986). Intracellular fluoride alters the kinetic properties of calcium currents facilitating the investigation of synaptic events in hippocampal neurons. *Journal of Neuroscience* **6**, 2915–2920.

KISKIN, N. I., KRISHTAL, O. A. & TSYNDRENKA, A. Y. (1986). Excitatory amino acid receptors in hippocampal neurons: Kainate fails to desensitize them. *Neuroscience Letters* **63**, 225–230.

KOSTYUK, P. G., KRISHTAL, D. A. & PIDOPLICHKO, V. I. (1975). Effects of internal fluoride and phosphate on membrane currents during intracellular dialysis of nerve cells. *Nature* **257**, 691–693.

LESTER, R. J., QUARUM, M. L., PARKER, J. D., WEBER, E. & JAHR, C. E. (1989). Interaction of 6-cyano-7-nitroquinoxaline-2,3-dione (CNQX) with the *N*-methyl-D-aspartate (NMDA) receptor-associated glycine binding site. *Molecular Pharmacology* **35**, 565–570.

MCCARREN, M. & ALGER, B. E. (1985). Use-dependent depression of i.p.s.p.s in rat hippocamal pyramidal cells *in vitro*. *Journal of Neurophysiology* **53**, 557–571.

MAGLEBY, K. L. & STEVENS, C. F. (1972). A quantitative description of end-plate currents. *Journal of Physiology* **223**, 173–197.

MALENKA, R. C., AYOUB, G. S. & NICOLL, R. A. (1987). Phorbol esters enhance transmitter release in rat hippocampal slices. *Brain Research* **403**, 198–203.

MAYER, M. L. (1989). Activation and desensitization of glutamate receptors in mammalian CNS. In *Ion Transport*, ed. BENHAM, C. D. & KEELING, D. J. Academic Press, New York (in the Press).

MAYER, M. L. & VYKLICKY, L. JR (1989). Concanavalin A selectively reduces desensitization of mammalian neuronal quisqualate receptors. *Proceedings of the National Academy of Sciences of the USA* **86**, 1411–1415.

MAYER, M. L. & WESTBROOK, G. L. (1984). Mixed-agonist action of excitatory amino acids on mouse spinal cord neurones under voltage clamp. *Journal of Physiology* **354**, 29–53.

MAYER, M. L. & WESTBROOK, G. L. (1985). The action of *N*-methyl-D-aspartic acid on mouse spinal neurones in culture. *Journal of Physiology* **361**, 65–90.

MAYER, M. L. & WESTBROOK, G. L. (1987). The physiology of excitatory amino acids in the vertebrate central nervous system. *Progress in Neurobiology* **28**, 197–276.

MAYER, M. L., WESTBROOK, G. L. & GUTHRIE, P. B. (1984). Voltage-dependent block by Mg^{2+} of NMDA responses in spinal cord neurones. *Nature* **309**, 263.

MONAGHAN, D. T., NGUYEN, L. & COTMAN, C. W. (1986). The distribution of [^{3}H]kainate binding sites in primate hippocampus is similar to the distribution of both Ca^{2+}-sensitive and Ca^{2+} insensitive [^{3}H]kainate binding sites in rat hippocampus. *Neurochemical Research* **11**, 1073–1082.

MULLER, D., JOLY, M. & LYNCH, G. (1988). Contributions of quisqualate and NMDA receptors in the induction and expression of LTP. *Science* **242**, 1694–1697.

NELSON, P. G., PUN, R. Y. K. & WESTBROOK, G. L. (1986). Synaptic excitation in cultures of mouse spinal cord neurones: receptor pharmacology and behaviour of synaptic currents. *Journal of Physiology* **372**, 169–190.

NOWAK, L., BREGESTOVSKI, P., ASCHER, P., HERBET, A. & PROCHIANTZ, A. (1984). Magnesium gates glutamate-activated channels in mouse central neurones. *Nature* **307**, 462–465.

PERKEL, D. H. & PERKEL, D. J. (1985). Dendritic spines: role of active membrane in modulating synaptic efficacy. *Brain Research* **325**, 331–335.

PETERFREUND, R. A. & VALE, W. W. (1983). Phorbol diesters stimulate somatostatin secretion from cultured brain cells. *Endocrinology* **113**, 200–208.

POZZAN, T., GATTI, G., DOZIO, N., VICENTINI, L. M. & MELDOLESI, J. (1984). Ca^{2+}-dependent and -independent release of neurotransmitters from PC12 cells: a role for protein kinase C activation? *Journal of Cell Biology* **99**, 628–638.

RALL, W. & SEGEV, I. (1985). Space clamp problems when voltage clamping branched neurons with intracellular microelectrodes. *Voltage and Patch Clamping with Microelectrodes*, ed. SMITH, T. G., LECAR, H., REDMAN, S. J. & GAGE, P. W., pp. 191–215. America Physiological Society, Bethesda, MD, USA.

RINK, T. J., SANCHEZ, A. & HALLAM, T. J. (1983). Diacylglycerol and phorbol ester stimulate secretion without raising cytoplasmic free calcium in human platelets. *Nature* **305**, 317–319.

SHAPIRA, R., SILBERBERG, S. D., GINSBERG, S. & RAHAMIMOFF, R. (1987). Activation of protein kinase C augments evoked transmitter release. *Nature* **325**, 58–60.

TANG, C.-M., DICHTER, M. & MORAD, M. (1989). Quisqualate activates a rapidly inactivating high conductance ionic channel in hippocampal neurons. *Science* **243**, 1471–1477.

TRUSSELL, L. O. & FISCHBACH, G. D. (1989). Glutamate receptor desensitization and its role in synaptic transmission. *Neuron* **3**, 209–211.

TRUSSELL, L. O., THIO, L. L., ZORUMSKI, C. F. & FISCHBACH, G. D. (1988). Rapid desensitization of glutamate receptors in vertebrate central neurons. *Proceedings of the National Academy of Sciences of the USA* **85**, 4562–4566.

WAKADE, A. R., MALHOTRA, R. K. & WAKADE, T. D. (1985). Phorbol ester, an activator of protein kinase C, enhances calcium-dependent release of sympathetic neurotransmitter. *Naunyn-Schmiedeberg's Archives of Pharmacology* **331**, 122–124.

WATKINS, J. C. & EVANS, R. H. (1981). Excitatory amino acid transmitters. *Annual Review of Pharmacology and Toxicology* **21**, 165–204.

WESTBERG, E., MONAGHAN, D. T., KALIMO, H., COTMAN, C. W. & WIELOCK, T. W. (1989). Dynamic changes in excitatory amino acid receptors in the rat hippocampus following transient cerebral ischemia. *Journal of Neuroscience* **9**, 798–806.

WIGSTRÖM, H. & GUSTAFSSON, B. (1985). Facilitation of hippocampal long-lasting potentiation by GABA antagonists. *Acta physiologica scandanavica* **125**, 159–172.

WIGSTRÖM, H. & GUSTAFSSON, B. (1988). Presynaptic and postsynaptic interactions in the control of hippocampal long-term potentiation. In *Long-Term Potentiation: From Biophysics to Behavior*, ed. LANDFIELD, P. W. & DEADWYLER, S. A., pp. 73–107. Alan R. Liss, Inc., New York.

ZUCKER, R. S. (1989). Short term synaptic plasticity. *Annual Review of Neuroscience* **12**, 13–31.

ZURGIL, N. & ZISAPEL, N. (1985). Phorbol ester and calcium act synergistically to enhance neurotransmitter release by brain neurons to culture. *FEBS Letters* **185**, 257–261.